RSC Advances

Construction and application of β-N-oxalyl-L-2,3-diaminopropanoic acid biosensor based on carboxylated multiwalled carbon nanotubes/gold nanoparticles/chitosan/Au electrode

Journal:	*RSC Advances*
Manuscript ID:	RA-ART-06-2014-005977.R1
Article Type:	Paper
Date Submitted by the Author:	23-Jul-2014
Complete List of Authors:	Batra, Bhawna; MDU, Rohtak,India, Pundir, C. S.; MD University, Biochemistry

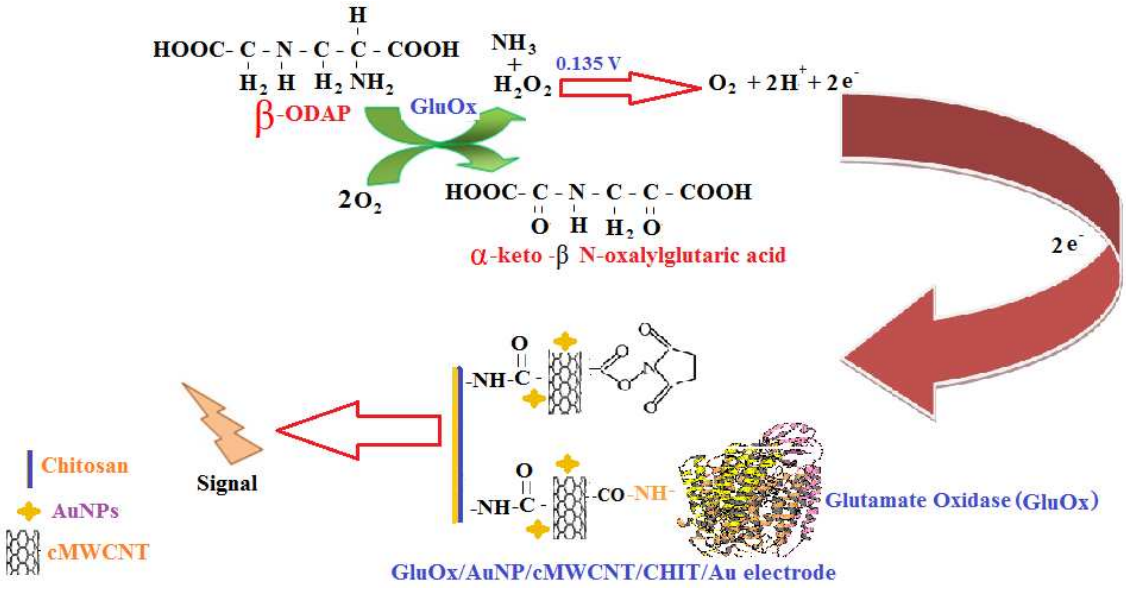
β-ODAP
GluOx
0.135 V
α-keto -β N-oxalylglutaric acid
2 e⁻
Chitosan
AuNPs
cMWCNT
Signal
Glutamate Oxidase (GluOx)
GluOx/AuNP/cMWCNT/CHIT/Au electrode

Construction and application of β-(3-N-oxalyl-L-2,3-diaminopropanoic acid biosensor based on carboxylated multiwalled carbon nanotubes/gold nanoparticles/chitosan/Au electrode

Bhawna Batra and C.S. Pundir*

Department of Biochemistry, M.D.University, Rohtak-124001, India

Running Title: Amperometric β-ODAP biosensor

*Corresponding author at: Department of Biochemistry, M D University, Rohtak-124001, Haryana, India. Tel.: +91 9416492413

E-mail address: pundircs@rediffmail.com

Abstract

We describe the construction of a new enzyme electrode (glutamate oxidase/carboxylated multiwalled carbon nanotubes/gold nanoparticles/chitosan/gold electrode: GluOx/cMWCNT/AuNPs/CHIT/Au) and its application for amperometric determination of β-ODAP (3-N-oxalyl-L-2,3-diaminopropanoic acid) in *Lathyrus* seeds. The enzyme electrode was characteirized by cyclic voltammetry (CV), electrochemical impedance spectroscopy (EIS), scanning electron microscopy (SEM) and fourier transform Infra-red spectroscopy (FTIR). The biosensor showed optimum response within 2s at pH 7.5 and 35 °C, when operated at 0.135 V. A good linear relationship was observed between the biosensor response i.e. current (mA) and L-glutamate (Glu) concentration in the range 2-550 μM. The biosensor had a detection limit of 2.32 μM with a high sensitivity of 486.31μA $cm^{-2}\mu M^{-1}$. The biosensor measured β-ODAP in glutamate free *Lathyrus* seed extract. The results for ODAP were correlated well (r = 0.9969) with those by standard colorimetric method. The enzyme electrode lost only 35% of its initial activity after its 70 regular uses over a period of 90 days.

Keywords: Carbon nanotube, Chitosan, Gold nanoparticles, Glutamate Oxidase, β-ODAP, *Lathyrus sativus*

Introduction

β-ODAP (3-N-oxalyl-L-2,3-diaminopropanoic acid or β-N-oxalyl-L-α,β-diaminopropanoic acid) a neurotoxin occurs in the seeds of grass pea (*Lathyrus sativus* L. family Fabaceae syn Leguminosae) which is a high-yielding, drought resistant legume [1, 2]. The grass pea seeds are consumed as a food in Northern India and neighboring countries as well as in Ethiopia. However, grass pea could not be developed as an important food legume due to the presence of this neurotoxin in the seeds. The consumption of Lathyrus seeds in large quantities for a prolonged period, can cause neurolathyrism which is characterized by spastic paraparesis involving the lower limbs almost exclusively[3-5].

Inspite of its neurotoxicity, β-ODAP has several physiological functions in grass pea such as carrier molecule for zinc-ions[6], as scavenger for hydroxyl ions[7] and as protector of photosynthesis at high light intensity[8]. ODAP naturally exits in the plant in two isomeric forms, the α-N-oxalyl derivatives, but only the β-isomer is toxic. The content of β-ODAP in the seeds of *L. sativus* has been reported in the range of 0.5-2.5%. The safe concentration of ODAP for human consumption is lower than 0.2% [9].

Hence determination of β-ODAP in *Lathyrus* seeds is very important. Various analytical methods such as colorimetric[10], flow injection analysis[11], high performance liquid chromatography (HPLC)[12], reversed-phase high performance liquid chromatography[13], Capillary zone electrophoresis[14,15] paper chromatography, liquid chromatography with precolumn derivatization with 1-fluoro- 2,4-dinitrobenzene[16] and 6-aminoquinolyl-N-hydroxysuccinimidyl carbamate (AQC)[17] and high pressure thin layer chromatography (HPTLC)[18] have been reported for determination of β-ODAP in grass pea seeds. However all these methods suffered from glutamate interference. Either liquid chromatography (LC)[19, 20] or enzymatic method using glutamate decarboxylase[21] were employed to remove glutmate

interference but it was time consuming, expensive and complicated due to enzyme/protein. Further, most of these methods did not satisfy the requirements for a simple, fast, accurate and specific method. Nevertheless, biosensing methods have many advantages over these methods, because of their simplicity, rapidity, high sensitivity and specificity. These β-ODAP biosensors were based on graphite rod modified with $Os^{2+/3+}$ [21], graphite electrode[20], Screen printed carbon electrode modified with MnO_2[21], Os containing mediating polymer, poly (ethyleneglycol) diglycidyl ether[22] and prussian blue modified GC electrode[23]. However, these electrodes suffered from limited electron communication, complexity of immobilization and low stability of enzymes. The use of nanomaterials in construction of a biosensor has offered great opportunities to improve their sensitivity, stability and anti-interference ability. Recently, carbon nanotubes (CNTs) have also been incorporated into transducers of electrochemical sensors due to their high surface-to-volume ratios and chemical functionalization. These CNT-based sensors have shown comparatively higher sensitivities, lower limits of detection, and faster electron transfer kinetics[24]. Among the metallic nanomaterials employed in biosensors, gold nanoparticles (AuNPs) have received greatest attention, due to their high surface-to-volume ratio and high surface energy which allow a stable immobilization of biomolecules and ability to permit fast and direct electron transfer between a wide range of electroactive species and electrode materials[25]. Chitosan (CHIT), a cationic polysaccharide with abundant amines has excellent film-forming ability, good biocompatibility and adhesion, and thus employed as an excellent matrix for immobilization of enzyme to fabricate enzyme electrodes[26].

The present report describes a new strategy for removal of L-glutamate from *Lathyrus* seed extract and construction of a novel enzyme electrode comprising glutamate oxidase immobilized onto carboxylated multiwalled carbon nanotubes/gold nanoparticles/chitosan

composite film electrodeposited on Au electrode[27] for amperometric determination of β-ODAP.

2. Experimental

2.1. Materials

L-Glutamic acid, gold chloride ($HAuCl_4$), N-ethyl-N'-(3-dimethylaminopropyl) carbodiimide (EDC), N-hydroxy succinimide (NHS), CHIT from SISCO Research Lab., Mumbai, India, carboxylated multi-walled carbon nanotubes (cMWCNT) (Functionalized MWCNT) from Intelligent Materials Pvt. Ltd. Panchkula (Haryana) India, GluOx, anion exchanger "Dowex® 1 X 8 chloride form" (mesh size : 50-100) from Sigma–Aldrich St. Louis, USA, were used. Grass pea (*Lathyrus sativus*) seeds were purchased from open market of Bhagalpur (Bihar). Double distilled water (DW) was used throughout the experimental studies.

2.2. Apparatus

UV Spectrophotometer (Shimadzu, Model 160 A), X-ray diffractometer (XRD), (122 Rigaku, D/Max2550, Tokyo, Japan), Transmission electron microscope (TEM (JEOL 2100 F), Dynamic light scaterring (DLS) (Zeatasizer, Malvern), Scanning electron microscope (SEM) (Zeiss EV040), Fourier transform Infra-red spectrophotometer (FTIR) (Thermo Scientific, USA). Potentiostat/Galvanostat (Autolab, model: AUT83785, manufactured by Eco Chemie) with a three electrode system composed of a Pt wire as an auxillary electrode, an Ag/AgCl electrode as reference electrode and GluOx/cMWCNT/AuNP/CHIT modified Au electrode as a working electrode, were used.

2.3. Construction of GluOx/cMWCNT/AuNP/CHIT modified Au electrode

2.3.1. Preparation of AuNP

AuNPs were prepared as described[28] with slight modification. Briefly, 100 ml aqueous $HAuCl_4$ (0.01%) was brought to boil on a temperature controlled magnetic stirrer and 2.5 ml 1% trisodium citrate solution was added to it with vigorous stirring until wine red coloured

colloidal gold nanoparticles (AuNPs) suspension was obtained. These AuNPs suspension was stored in dark glass bottle at 4°C until use.

2.3.2. Characterization of AuNPs

AuNPs were characterized by UV and visible spectroscopy and XRD at Department of Physics, Guru Jambheshwar University, Hisar, Haryana (India), TEM at Jawahar Lal Nehru Universuty, New Delhi on commercial basis and DLS at Amity Institute of Nanotechnology, Amity University, Noida, India.

2.3.3. Electrodeposition of cMWCNT/AuNP/CHIT onto Au electrode

One milligram of c-MWCNT was suspended into 4 ml mixture of concentrated H_2SO_4 and HNO_3 in 3:1 ratio and ultrasonicated for 2 h to obtain a homogeneous mixture. The dispersed cMWCNT solution (0.1ml) was mixed into a mixture of 0.5 ml EDC (0.2 M) and 0.5ml NHS (0.2 M), its pH was adjusted to 6.0 and kept at room temperature for 1 hr. The surface of a Au electrode (0.30 cm^2) was polished manually by alumina slurry (diameter 0.05µm) with a polishing cloth, washed thoroughly with DW, placed into ethanol, sonicated to remove adsorbed particles and finally washed with DW (3-4 times). CHIT (0.5% in acetic acid, 200µl) was added to 25 ml 1M KCl and electrodeposited onto Au electrode through cyclic voltammetry using galvanostat applying 20 successive deposition cycles between - 0.15 to 0.20 V at a scan rate of 20 mV/s. AuNPs suspension (200 µl) and 400 µl of EDC and NHS treated cMWCNT suspension were added into 25 ml 1M KCl to get a mixture of cMWCNT and AuNPs. The mixture was electrodeposited onto the CHIT modified Au electrode in an electrochemical cell system applying 20 deposition cycles between –0.1 to 0.2 V at scan rate of 20 mV/s. During the electrochemical polymerization, the surface of Au wire became green gradually, indicating the deposition of cMWCNT-AuNPs onto CHIT film modified Au wire. The resulting cMWCNT/AuNPs/CHIT modified gold electrode was washed thoroughly with DW to remove unbound matter and kept in a dry Petri-plate at 4^oC.

2.3.4. Immobilization of GluOx onto cMWCNT/AuNP/CHIT modified Au electrode

cMWCNT/AuNPs/CHIT/Au electrode was placed into 2ml of sodium phosphate buffer (0.1M, pH 7.4) containing 100 µl of GluOx (2.3 U/ml) and kept overnight at 4°C for immobilization. The resulting bioelectrode (GluOx/cMWCNT/AuNPs/CHIT/Au electrode) was washed 3-4 times with 0.1 M sodium phosphate buffer, pH 7.4 to remove unbound enzyme and used as working electrode . It was stored at 4^{o}C, when not in use.

2.3.5. Characterization of GluOx/cMWCNT/AuNPs/CHIT/Au electrode

The fabricated enzyme electrode was characterized by scanning electron microscopy (SEM), Fourier transform infrared (FTIR) spectroscopy and electrochemical impedance spectroscopy (EIS).

To investigate the morphology of cMWCNT/AuNPs/CHIT/Au electrode with and without immobilized enzymes, the electrodes were cut into small pieces (1 cm) and placed on a specimen chamber of 2 cm diameter using a spray gun, generally mounted rigidly on a specimen holder called a specimen stub and their images were taken in a scanning electron microscope.

To record FTIR spectra of enzyme electrode at different stages of its construction, the deposited material was scrapped off the Au electrodes, grinded with dry potassium bromide (KBr) and then this powder was pressed in a mechanical press to form a translucent pellet through which the beam of the spectrometer could pass. The pellet was kept in the socket of FTIR spectrophotometer and its spectrum was recorded.

The EIS studies of enzyme electrode before and after immobilization were carried out in a Potentiostat/Galvanostat equipped with FRA in the frequency range, 0.01 to 105 Hz, amplitude 5 mV, after dipping the three electrodes system in 0.05 M PB (pH 7.5) containing 5 mM $K_3Fe(CN)_6/K_4Fe(CN)_6$ (1:1) as a redox probe. During an impedance measurement, a

FRA was used to impose a small amplitude AC signal to the electrode via the load. The AC voltage and current response of the electrode was analyzed by the FRA to determine the resistive, capacitive and inductive impedance behaviour of the electrode at that particular frequency.

2.3.6. Cyclic voltametric measurements and testing of β-ODAP biosensor

Cyclic voltammogram (CV) of GluOx/cMWCNT/AuNPs/CHIT/Au electrode was recorded in galvanostat between −0.1 to 0.6 V vs Ag/AgCl as reference and Pt wire as counter electrode in 30 ml 0.1 M sodium phosphate buffer (pH 7.4) containing 1 mM Glu (100 µl). The maximum response was observed at 0.135 V and hence subsequent amperometric studies were carried out at this voltage.

2.4. Optimization of β-ODAP biosensor

To determine optimum pH, the pH of reaction buffer was varied from 5.0 to 10.0 at an interval of 0.5 each at a final conc. of 0.1 M: sodium acetate buffer for pH 5.0 to 6.0, sodium phosphate buffer pH 6.5 to 7.5, Tris-HCl buffer pH 8.0 to 9.0 and glycine buffer pH 9.5 to 10.0. Similarly optimum temperature was studied by incubating the reaction mixture at different temperature (20–50°C) and time (1–40 s). The effect of Glu concentration on biosensor response was determined by varying its concentration from 2µM to 700µM.

2.5. β-ODAP determination in seed extract by GluOx/cMWCNT/AuNPs/CHIT/AuE

The grass pea (*Lathyrus sativus*) seeds (400 g) were ground to powder and then homogenised in DW (2 l) in a pestle and mortar at room temperature (25°C). The homogenate/slurry was kept at 60-65°C for 15 hr with occasional stirring for evaporation of DW and then passed through filter paper. The residue from the filtered slurry was further extracted with DW (1 l). The combined water extracts were treated with alcohol to achieve 75 % concentration, stirred,

and filtered after half an hour. The filtrate was concentrated under reduced pressure to about 1.5 liters. The concentrate was extracted first with ether (1 liter) and subsequently with chloroform (1 liter)[1]. Then aqueous phase was separated and loaded onto a Dowex column (r × h = 0.5 cm × 25 cm) pre-equiliberated with sodium phosphate buffer (pH 2.5, 0.1 M). The column was washed in the same buffer. The column was eluted using a linear gradient of 0.1 M-0.8 M KCl and fractions (1 ml) each were collected at a flow rate of 0.5 ml/min. Each fraction was analysed amperometrically for β-ODAP using the present biosensor in the similar manner as described above for its testing/response measurement, under its optimal working conditions except that Glu was replaced by fraction. A plot between fraction no. and current response was drawn and total current response was calculated from the area of peak for β-ODAP (Fig. 1). The β-ODAP concentration was interpolated from a standard curve of Glu concentrations v/s current prepared under optimal conditions (Fig. 2).

⟶ Insert Fig.1& 2 here

2.6. Interference study

The following interferents such as cysteine, methionine, lysine, aspartic acid, glycine, histidine, leucine, isoleucine, asparagine, proline, phenylalanine, valine, threonine, tyrosine, tryptophan, arginine, serine, alanine were added individually in the reaction mixture each at a final concentration of 1mM. The biosensor response i.e. current (μA) was measured and compared with that where none was added (control) and % relative response was calculated considering the control as 100 %.

2.7. Reusability and storage stability of GluOx/cMWCNT/AuNPs/CHIT/Au electrode

To reuse the working electrode, it was washed by dipping it in 0.1 M, pH 7.5 sodium phosphate buffer. The long-term storage and stability of the biosensor was investigated over a 3 months period, when enzyme electrode was stored in a refrigerator at 4 °C in 0.1 M PB, pH

7.5.

3. Results and discussion

3.1. Characterization of AuNPs

AuNPs were characterized by UV and visible spectroscopy, XRD, TEM and DLS (Fig. 3 A, B, C, & D). UV and visible spectra showed strong absorbance peak at 560 nm, confirming the synthesis of AuNP (Fig. 3A). The XRD patterns of AuNPs depicted a well defined diffraction pattern, which was in agreement with JCPDS card No. 089-3697. (Fig. 3 B). The spherical shape of AuNPs with an average size of 20 nm was confirmed by TEM images (Fig. 3 C). DLS utilizes temporal variations of fluctuations of the scattered light to measure an average hydrodynamic diameter of particles suspended in a liquid medium. AuNPs are extraordinary light scatterers at or near their surface plasmon resonance wavelength. The dynamic light scattering provided the diameter of the gold nanoparticles as 78.5 nm which might be due to their aggregation (Fig. 3 D).

→ Insert Fig. 3 here

3.2. Morphological characterization of Au electrode by SEM studies

Fig.4 shows the stepwise modification of electrode. The SEM image of the bare Au electrode showed uniform morphology (Fig. 4a). SEM image of cMWCNT/AuNP/CHIT/Au exhibited homogenous and cable-like morphology of the nanostructure of cMWCNT/AuNP/CHIT/Au composite film, which showed that c-MWCNTs were well dispersed in the composite film (Fig. 4b). After immobilization of GluOx on cMWCNT/AuNP/CHIT/Au composite film, the hybrid bioelectrode showed the sporadic appearance of beaded structure, indicating that GluOx was successfully immobilized on the surface of c-MWCNT/PANI composite film (Fig. 4c)

→ Insert Fig. 4 here

3.3. Fourier transforms infrared (FTIR) spectroscopy

Fig.5 (A) showed FTIR spectra for CHIT/Au electrode (curve i), cMWCNT/AuNP/CHIT/Au electrode (curve ii) and GluOx/cMWCNT/AuNP/CHIT/Au electrode (curve iii) [27]. FTIR spectra of electrodeposited CHIT/Au composite showed peak at 1745 cm^{-1} due to C-O stretching. The peak at 1650 cm^{-1} can be attributed to C-O stretching along with N-H deformation mode and 1096 cm^{-1} to the stretching vibration mode of the hydroxyl group. Curve (ii) showed the FTIR spectra of cMWCNT/AuNP/CHIT/Au electrode, revealing several significant peaks. The peak at the 1558 cm^{-1} corresponded to the stretching mode of the C=C double bond that formed the framework of the carbon nanotube sidewall. The peak at 1730 and 1028 cm^{-1} corresponded to the stretching modes of -COOH groups. FTIR spectrum of GluOx/cMWCNT/AuNP/CHIT/Au bioelectrode (curve iii) showed the appearance of additional bands at 1695 cm^{-1} assigned to the carbonyl stretch indicating the covalent binding of GluOx with cMWCNT.

⟶ Insert Fig. 5 here

3.4. Electrochemical impedance measurements

EIS provides an effective method to probe electronic features of surface-modified electrodes. Fig. 6 shows Nyquist plots obtained for (a) bare Au electrode (b) cMWCNT/AuNP/CHIT/Au electrode and (c) GluOx/cMWCNT/AuNP/CHIT/Au electrode, respectively [27]. Nyquist diameter (real axis value at lower frequency intercept) indicated the value of charge transfer resistance (R_{CT}) i.e. hindrance provided by the electrode material to transfer charge from solution to the electrode which is correlated with the modification of the surface. The RCT value obtained for the GluOx/cMWCNT/AuNP/CHIT/Au electrode (curve (c), 570 Ω) was higher than that of the cMWCNT/AuNP/CHIT/Au electrode (curve (b), 400 Ω) which can be attributed to the insulating nature of GluOx that inhibits permeability of $[Fe(CN)_6]^{3-/4-}$ to the electrode surface.

→ Insert Fig. 6 here

3.5. Construction and response measurement of β-ODAP biosensor

An enzyme (GluOx) electrode was fabricated by immobilizing covalently GluOx from *Streptomyces* onto cMWCNT/AuNP/CHIT/Au electrode using EDC and NHS chemistry[27]. EDC was used to conjugate the free carboxyl (-COOH) groups of c-MWCNT to amine (-NH_2) groups of the GluOx, using NHS as a catalyst. Fig.7 showed a bigger redox peak of GluOx/cMWCNT/AuNP/CHIT/Au electrode than that of GluOx/cMWCNT/CHIT/Au electrode & GluOx/AuNPs/CHIT/Au electrode, which corresponded to the oxidation of Glu on the surface of the modified electrode as well as the enhancement of the current. It appeared that the cMWCNT/AuNP/CHIT/Au nanocomposite provided a biocompatible environment to the GluOx, cMWCNT and AuNPs act as an electron mediator, resulting in an accelerated electron transfer between enzyme and electrode.

→ Insert Fig. 7 here

During the response measurement of the present biosensor, GluOx catalyses the oxidation of β-ODAP into α-keto acid and H_2O_2 which is dissociated into $O_2 + 2H^+ + 2e^-$ at 0.135 V. These electrons flow through cMWCNT and AuNPs to Au electrode and generate the signal in the form of current.It appeared that the cMWCNT/AuNP/CHIT/Au nanocomposite provided a biocompatible environment to the enzyme, while cMWCNT and AuNPs acted as an electron mediator, resulting in an accelerated electron transfer between enzyme and electrode surface. All these electrochemical reactions are summarised in Fig. 7.

→ Insert Fig. 7 here

3.6. Optimization of biosensor

The experimental conditions affecting the biosensor response were studied in terms of effect of pH, incubation temperature and substrate (Glu) concentration. The biosensor showed optimum response i.e. current at pH 7.5 (Fig. 8 a), which is almost similar to that of earlier

biosensors (Table 1). The optimum incubation temperature for biosensor was 35ºC (Fig. 8 b). There was a hyperbolic relationship between electrode response and Glu concentration in the range 2-700 μM with a linearity in the range, 2-550 μM (Fig. 2), which is a better than those of earlier biosensors (Table 1). Similarly, the detection limit (LOD) of the present biosensor was 2.32 μM (S/N=3), which is also better/lower than that for earlier biosensors (Table 1). The lower LOD of present biosensor might be due to the film of carboxylated multiwalled carbon nanotubes and gold nanoparticles attached on to Au electrode through chitosan film, which provided high biocompatibility and fast electron transfer rate between the enzyme and electrode.

→ Insert Fig. 8 here

3.8 Determination of β-ODAP in seed extract

3.8.1. Preparation of glutamate free sample of Lathyrus seeds

A new method has been developed to remove glutamate interference from β-ODAP containing grass pea extract using Dowex 1 X 8, an anion exchanger. The removal was based on different isoelectric points of glutamate (pI = 3.22) and β-ODAP (pI = 2.02). When a sodium phosphate buffer (0.1 M, pH 2.5, pKa1= 2.12) was passed through this anion exchanger, glutamate and β-ODAP are acquire positive and negative charge respectively. At this stage, glutamate (positively charged at pH =2.5) passes through the column, while β-ODAP (negatively charged at pH =2.5) remains attached to the ion exchanger (positively charged at pH = 2.5) leading to the removal of glutamate from β-ODAP. The glutamate free sample containing β-ODAP was eluted from Dowex ion exchanger column in the same buffer using a continuous ionic gradient (0.1 M - 0.8 M KCl) and analysed for amperometric determination of β-ODAP by the present biosensor (Fig. 9). The present method for removal of glutamate interference is better than earlier LC method based on Carbopac anion exchange column[21] , as the former has no chance of mixing glutamate with β-ODAP, while the latter

method has such chances (due to closeness of elution peaks for glutamate and β-ODAP). The method is also far better than previous method which included the treatment of sample with a glutamate decarboxylase/protein, which is likely to undergo hydrolysis to generate interfering amino acids[23].

→ Insert Fig. 9 here

3.8. 2. Measurement of β-ODAP

The β-ODAP content in seed extract as measured by the present biosensor was 19.2 μM which amounts to 1.62 ± 0.06 g/Kg seed powder (mean ± SD) (on fresh weight basis). There was a good correlation (r = 0.9969) between these values and the values obtained by colorimetric method (Fig. 10).

→ Insert Fig. 10 here

3.9. Long-term stability of enzyme electrode

The enzyme electrode lost 35% of its initial activity after its 70 regular uses over a period of 90 days. This stability of enzyme electrode is better than earlier enzyme electrodes (Table 1).

3.10. Interference study

Among the various substances tested such as cysteine, methionine, lysine, aspartic acid, glycine, histidine, leucine, isoleucine, asparagine, proline, phenylalanine, valine, threonine, tyrosine, tryptophan, arginine, serine, alanine (each at 1mM), none had practically any interference on the present biosensor response.

4. Conclusion

A new method was developed for removal of glutamate interference in measurement of β-ODAP in *Lathyrus* seed extract, which is better than earlier reported methods. An improved β-ODAP biosensor was constructed based on a nanocomposite thin film of carboxylated multiwalled carbon nanotubes/gold nanoparticles/chitosan. The biosensor showed rapid response (2s), lower detection limit (2.32 μM), higher sensitivity (486.31μA/cm^2/μM),

broader working range (2-550 μM) and longer stability (3 months). This nanocomposite film also be used for improvement of other biosensors also.

Acknowledgement

Author (Bhawna Batra) is thankful to the Council of Scientific and Industrial Research (CSIR), India, for the award of Junior Research Fellowship during this study.

References

Y. Wang, J. Huang, C. Zhang, J. Wei and X. Zhou, Electroanalysis, 1998, 10, 776–778.

1. S.L.N. Rao, P. R. Adiga and P. S. Sarma, *Biochemistry,* 1964, 3, 432–436.

2. V.V.S. Murti, T. R. Seshadri and T. A. Venkitasubramanian, *Phytochemistry,* 1964, 3, 73–78.

3. H. Selye, *Rev. Can. Biol.,* 1957, 16, 1–2.

4. A.C. Ludolph, J. Hugon, M. P. Dwivedi, H. H. Schaumburg and P.S. Spencer, *Brain,* 1987, 110, 149–165.

5. P. S. Spencer, A. C. Ludolph and G. E. Kisby, *Environ. Res.,* 1993, 62, 106–113.

6. F. Lambein, R. Haque, J.K. Khan, N. Kebede and Y.H. Kuo, *Toxicon,*1994, 32, 461-466.

7. G. K. Zhou, Y. Z. Kong, K. R. Cui, Z. X. Li, Y. F. Wang, *Phytochemistry,*2001, 58, 759–762.

8. J. Zhang, G. M. Xing, Z. Y. Yan and Z. X. Li, *Russ. J. Plant Physiol.,* 2003, 50, 618–622.

9. P. S. Cheema, G. Padmanaban, P. S. Sarma, *J. Neurochem.,* 1971, 18, 2137-2144 .

10. S.L.N. Rao, *Anal. Biochem.,* 1978, 86, 386-395.

11. G. Moges and G. Johansson, *Anal. Chem.,* 1994, 66, 3834–3839.

12. A. Geda, C. J. Briggs and S. Venkataram, *J. Chromatogr.,* 1993, 635, 338–341.

13.G.E. Kisby, D. N. Roy and P.S. Spencer, *J. Neurosci. Meth.,* 1988, 26, 45–54.

14. A. M. K. Arentoft and B. N. Greirson, *J. Agric. Food Chem.,* 1995, 43, 942–945.

15. L. Zhao, X. G. Chen, Z. D. Hu, Q. F. Li, Q. Chen and Z. X. Li, *J. Chromatogr. A.,* 1999, 857, 295–302.

16. F. Wang, X. Chen, Q. Chen, X. Qin and Z. Li, *J. Chrom. A.,* 2000, 883, 113–118.

17. X. Chen, F. Wang, Q. Chen, X.C. Qin, Z.X. Li, *J. Agric. Food Chem.,* 2000, 48, 3383–3386.

18. M.M. Paradkar, R.S. Singhal and P. R. Kulkarni, *J. Sci. Food Agric.,* 2003, 83, 727–730.

19. A. Belay, T. Ruzgas, E. C. Regi, G. Moges, M. Tessema, T. Solomon and Lo Gorton, *Anal. Chem.,* 1997, 69, 3471-3475.

20. S. Marichamy, Y. Yigzaw, L. Gorton, B. Mattiasson, *J. Sci. Food Agric.,* 2005, 85, 2027–2032.

21. N. W. Beyene, H. Moderegger and K. Kalcher, *Electroanalysis,* 2004, 16, 268-274.

22. Y. Yigzaw, N. Larsson, L. Gorton, T. Ruzgas, T. Solomon, *J. Chrom. A.,* 2001, 929, 13–21.

23. S. Varma, Y. Yigzawa and L. Gorton, *Anal. Chim. Act.,* 2006, 556, 319-325.

24. C. B. Jacobs, M. J. Peairs and B. J. Venton, *Anal. Chim. Act.,* 2010, 662, 105–127.

25. Y. Lia, H. J. Schluesenerb and S. Xua, *Gold Bulletin,* 2010, 43, 29-41.

26. D. Feng, F. Wang and Z. Chen, *Sens. Act. B.,* 2009, 138, 539–544.

27. B. Batra and C.S. Pundir, *Biosens. Bioelectron.,* 2013, 47, 496-501.

28. Y. Zhang, K. Zhang, H. Ma, *Am. J. Biomed. Sci.,* 2009, 1, 115-125.

29. N. W. Beyene, H. Moderegger and K. Kalcher, *Lathyrus Lathyrism Newsletter,* 2003, 3, 47-49.

Table 1 Comparison of analytical properties of β-ODAP biosensors

Properties	Belay et al., 1997	Yigzaw et al., 2001	Yigzaw et al., 2002	Beyene et al., 2003	Beyene et al., 2004	Marichamy et al., 2005	Varma et al., 2006	Present work
Support of immobilization	Graphite rod modified with $Os^{2+/3+}$	Graphite rod modified with Os containing mediating polymer with poly (ethyleneglycol) diglycidyl ether	Graphite rod	Screen printed carbon electrode modified with MnO_2	Screen printed carbon electrode modified with MnO_2	Graphite electrode	Prussian blue modified GC electrode	cMWCNT/AuP/CHIT/Au
Optimum pH	7.0	7.5	7.5	7.75	7.75	7.5	7	7.5
Optimum voltage	-50 mV	-	-50 mV	-	440 mV	-50 mV	-50 mV	135 mV
Linearity	-	1-250 µM	1-250 µM	0.284-28.4 mM	195-1950 µM	1-600 µM	0.05-1 mM	2-550 µM
Detection limit	4µM	2 µM	2 µM	0.164 mM	111 µM	-	-	2.32 µM
Response time	-	10 min	10 min	-	-	-	-	2 s
Sensitivity	-	4.6 mA/M/cm^2	-	-	-	-	-	486.31 µA/µM/cm^2
Storage stability	-	2 days	2 days	65 days	40 days	-	-	90 days

Figure captions

Fig.1. Current response in different fractions of Lathyrus seed extract eluted from ion exchanger

Fig.2. (A) Calibration curve at a concentration 2-10 μM L-glutamate (B) Standard curve for L-Glutamate by β-ODAP biosensor based on GluOx/cMWCNT/AuNP/CHIT based Au electrode

Fig.3. (A) UV spectrum of AuNP (B) Transmission electron microscopic (TEM) image of AuNP (C) X-ray diffraction pattern of AuNP (D) Size distributions by dynamic light scattering (DLS)

Fig.4. SEM images of (a) bare Au electrode (b) cMWCNT/AuNP/CHIT/Au electrode (c) GluOx/cMWCNT/AuNP/CHIT/Au electrode

Fig.5. (A) FTIR spectra of CHIT/Au (i) cMWCNT/AuNP/CHIT/Au (ii) GluOx/cMWCNT-AuNP/CHIT /Au electrode (iii)

Fig.6. Impedance spectra of (a) bare Au electrode (b) cMWCNT/AuNP/CHIT/Au electrode and (c) GluOx/cMWCNT-AuNP/CHIT/Au electrode electrode in $[K_3Fe(CN)_6]$ (5 mM)

Fig.7. Cyclic voltamogram for (a) GluOx/AuNPs/cMWCNT/CHIT/Au (b) GluOx/cMWCNT/CHIT/Au electrode (c) GluOx/AuNP/CHIT/Au electrode in 30 ml 0.1 M sodium phosphate buffer (pH 7.4) containing 0.5 mM glutamic acid (100 μl); Scan rate: 20 mV/s.

Fig.8. Schematic diagram of β-ODAP biosensor

Fig.9. (a) Influence of applied pH on the current response of GluOx/cMWCNT-AuNP/CHIT/Au electrode. (b) Influence of applied temperature on the current response of GluOx/cMWCNT-AuNP/CHIT/Au electrode

Fig.10. β-ODAP concentration in fractions 1 to 6 (each 1.5 ml) as measured by β-ODAP biosensor

Fig.11. Correlation between β-ODAP values as determined by colorimetric method (x-axis) and present biosensor method employing GluOx/cMWCNT-AuNP/CHIT/Au electrode.

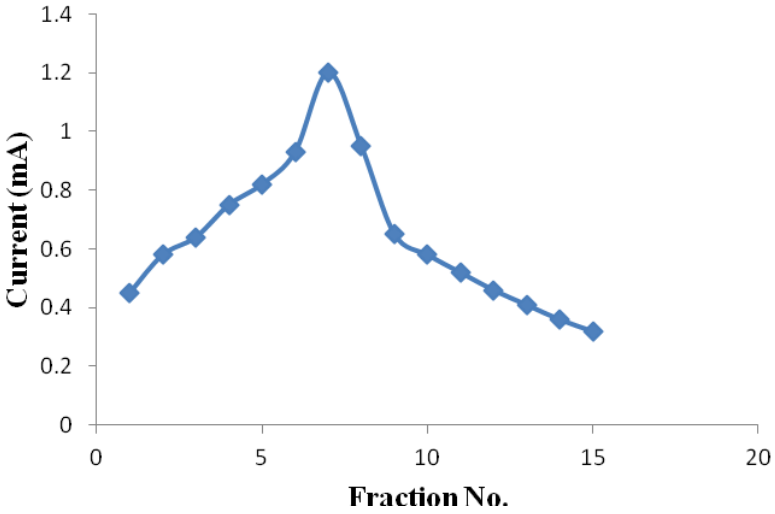

Fig.1.

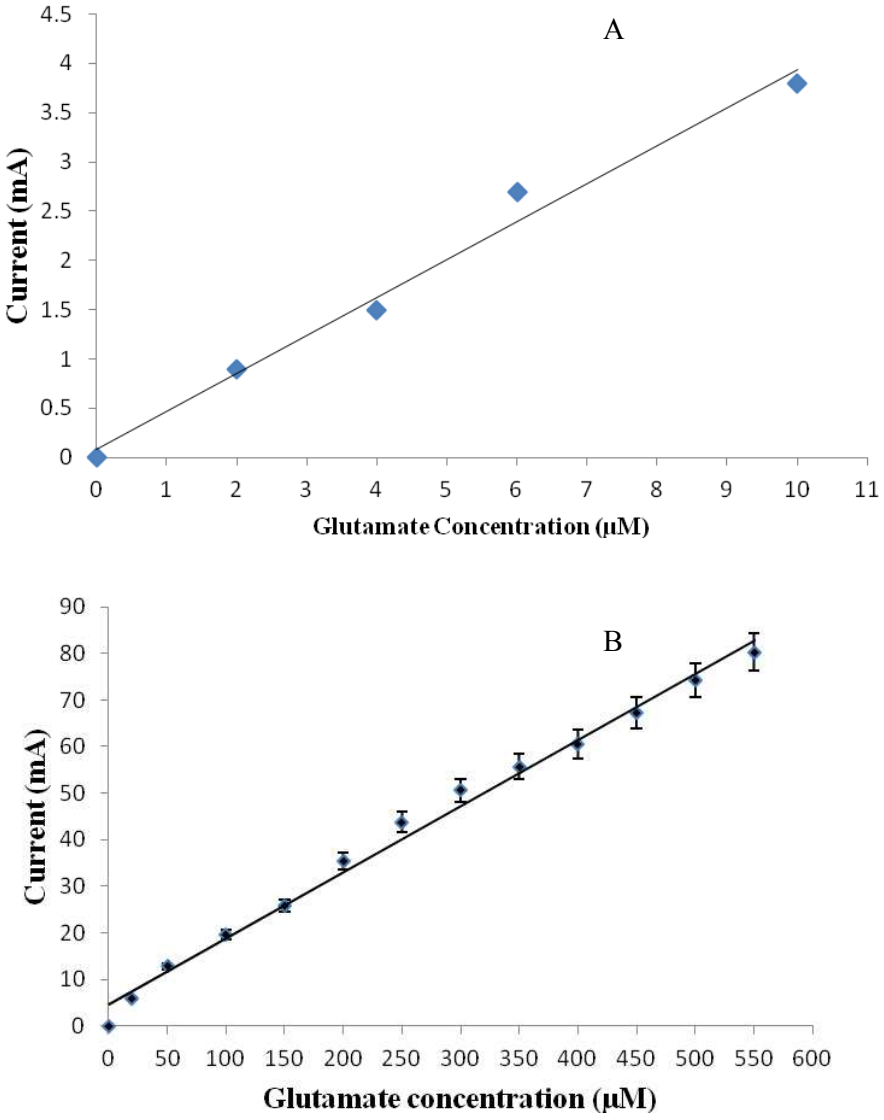
A
Current (mA)
Glutamate Concentration (µM)
B
Current (mA)
Glutamate concentration (µM)

Fig.2.

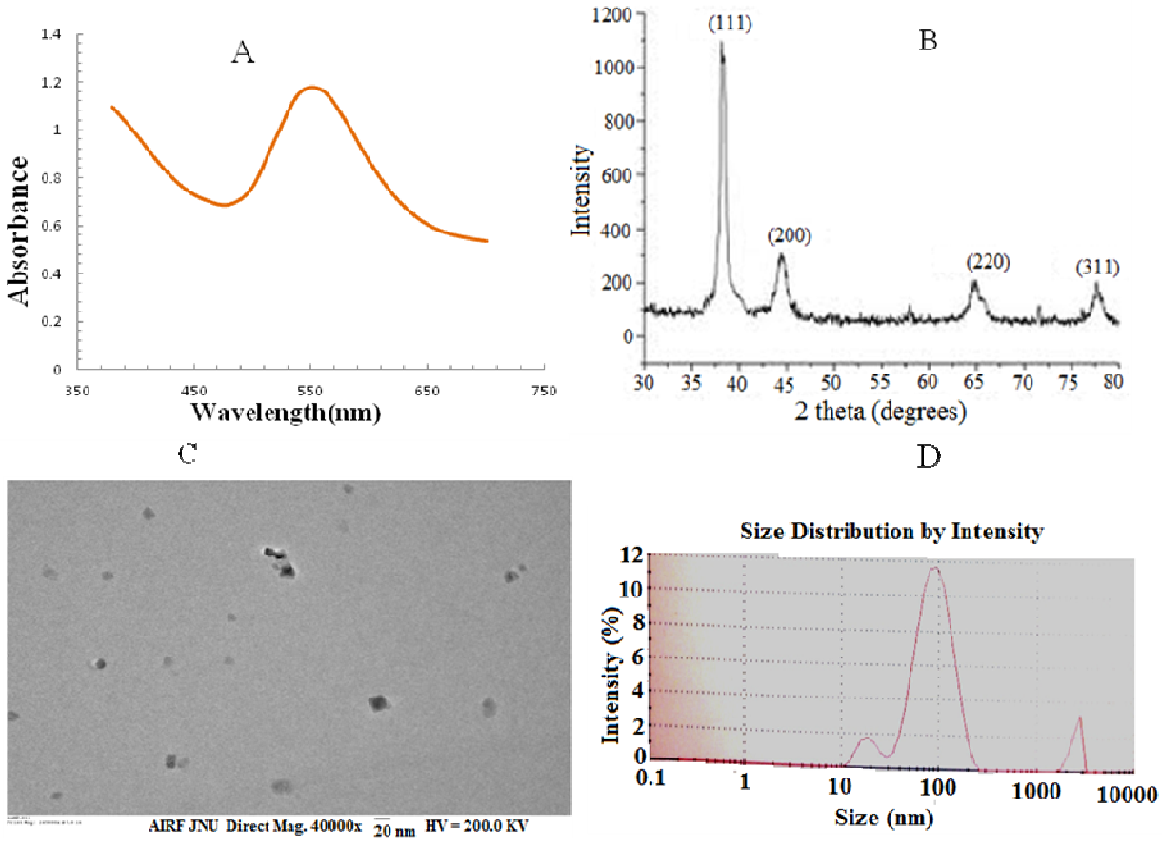
A
Absorbance
Wavelength(nm)
B
Intensity
(111)
(200)
(220)
(311)
2 theta (degrees)
C
AIRF JNU Direct Mag. 40000x 20 nm HV = 200.0 KV
D
Size Distribution by Intensity
Intensity (%)
Size (nm)

Fig.3.

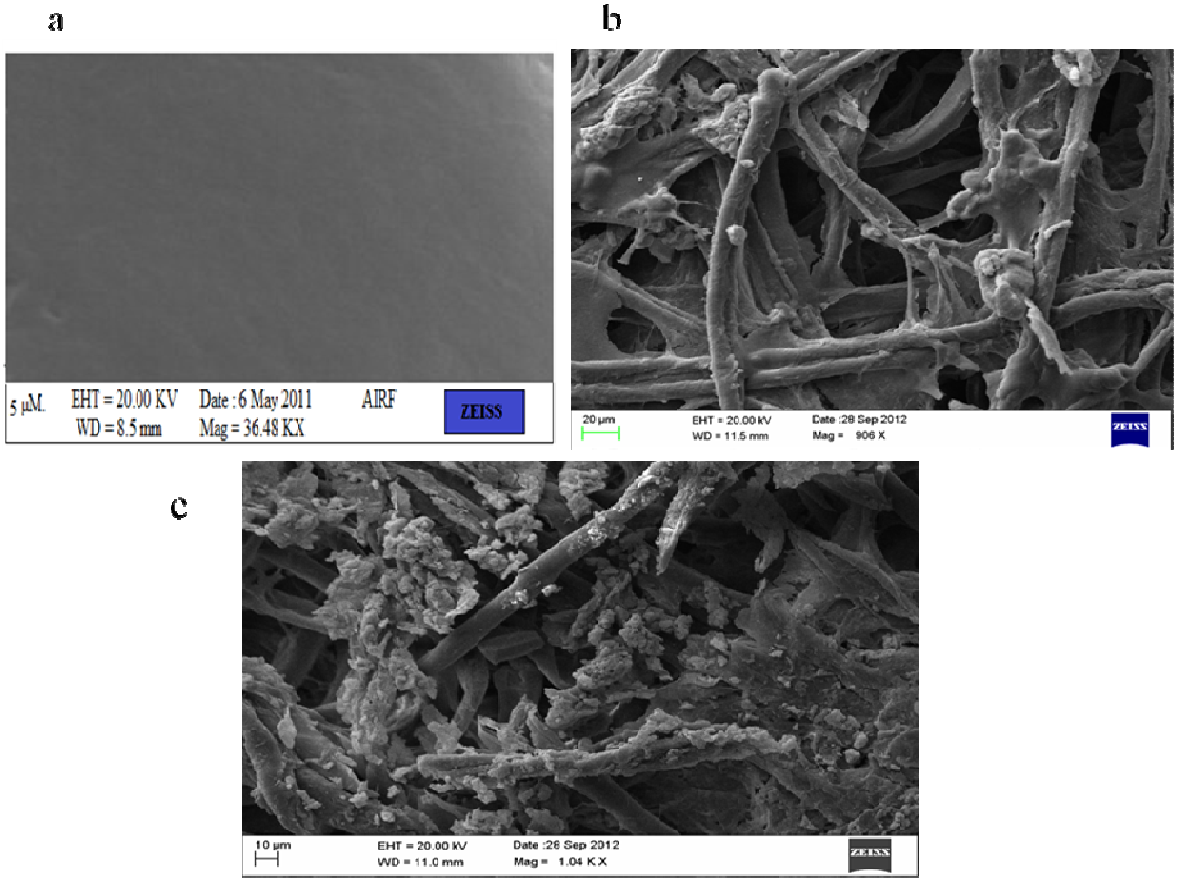
a
5 µM.
EHT = 20.00 KV
WD = 8.5 mm
Date : 6 May 2011
Mag = 36.48 KX
AIRF
ZEISS
b
20 µm
EHT = 20.00 kV
WD = 11.5 mm
Date :28 Sep 2012
Mag = 906 X
c
10 µm
EHT = 20.00 kV
WD = 11.0 mm
Date :28 Sep 2012
Mag = 1.04 K X

Fig. 4.

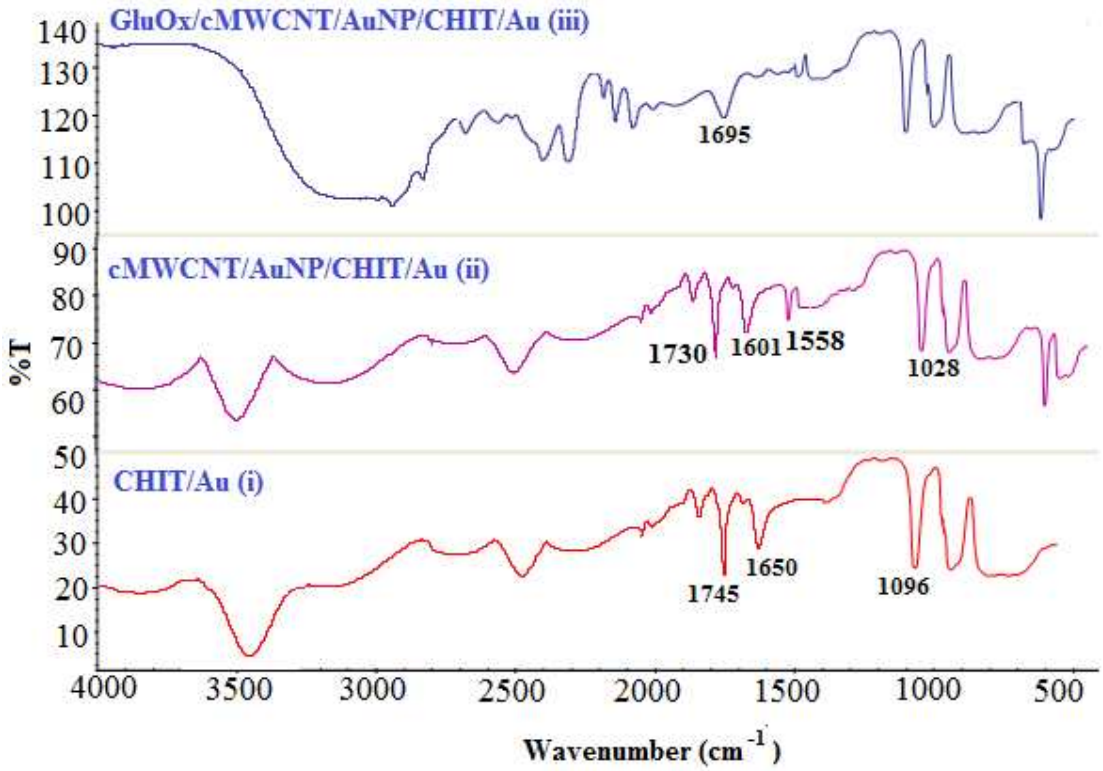
GluOx/cMWCNT/AuNP/CHIT/Au (iii)
1695
cMWCNT/AuNP/CHIT/Au (ii)
1730
1601
1558
1028
CHIT/Au (i)
1745
1650
1096
%T
Wavenumber (cm-1)

Fig.5.

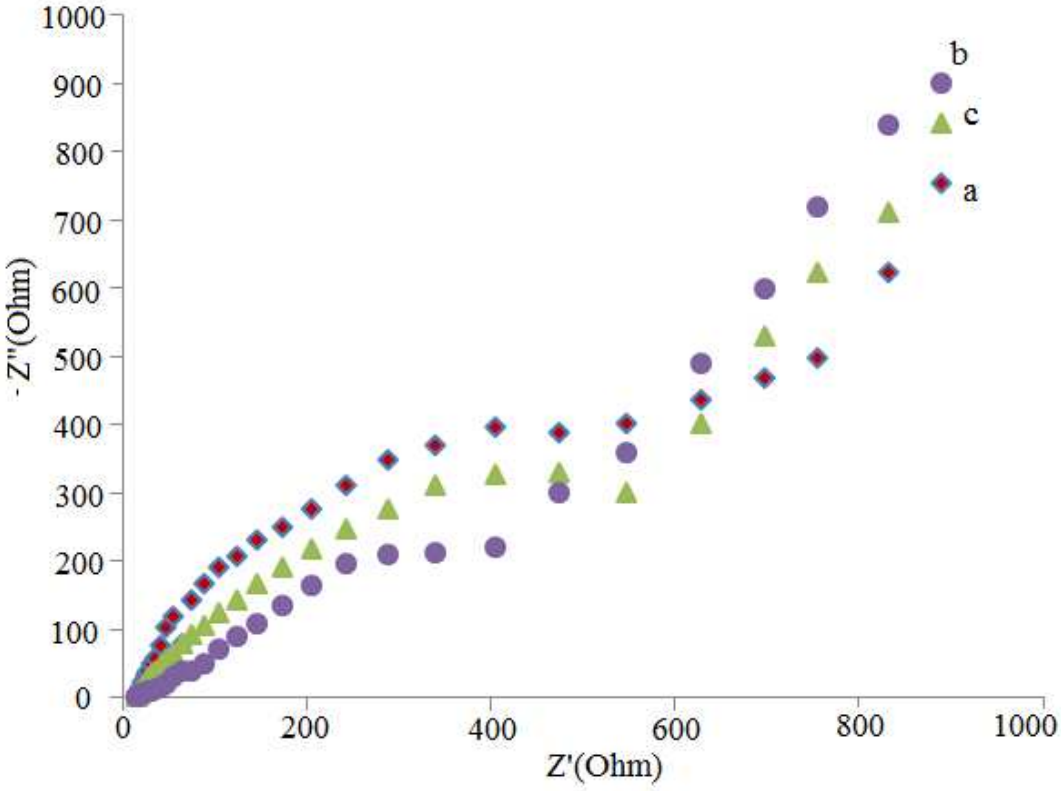
1000
900
800
700
600
500
400
300
200
100
0
-Z''(Ohm)
0
200
400
600
800
1000
Z'(Ohm)
b
c
a

Fig.6.

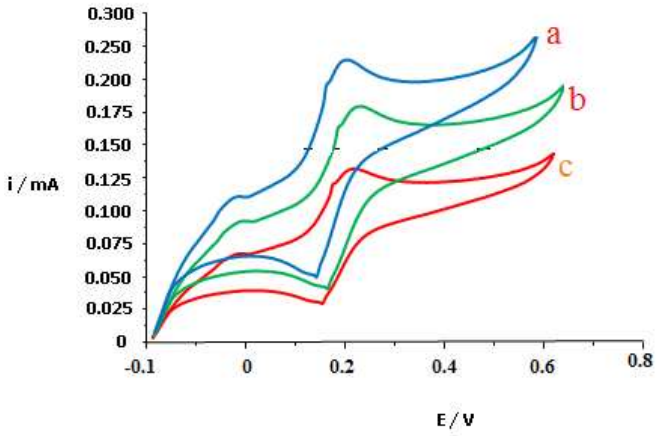
0.300
0.250
0.200
0.175
0.150
0.125
0.100
0.075
0.050
0.025
0
i / mA
-0.1
0
0.2
0.4
0.6
0.8
E / V
a
b
c

Fig.7.

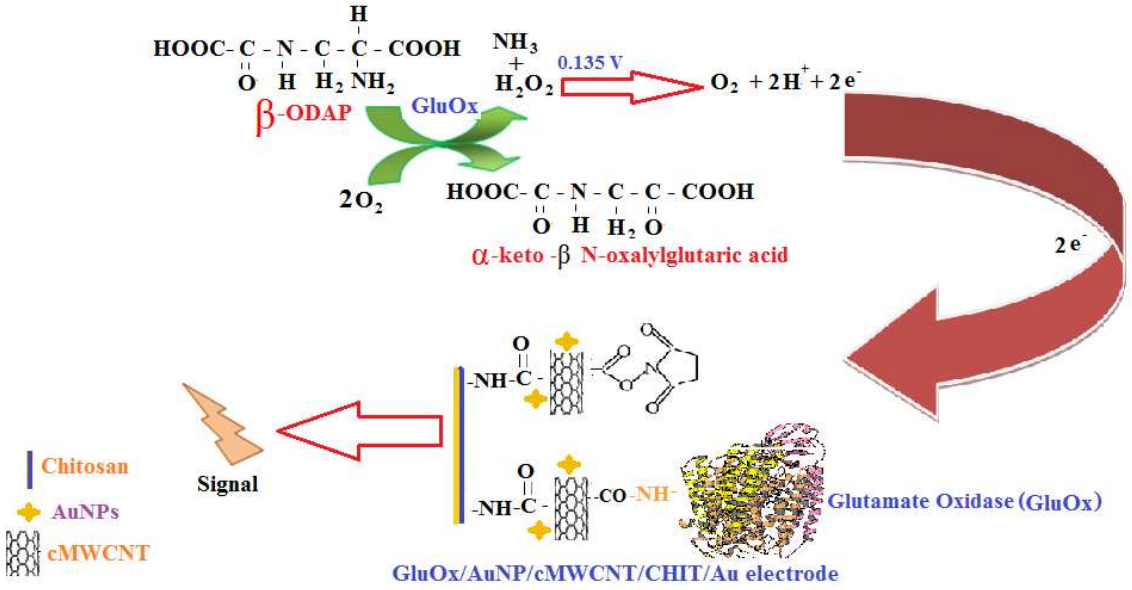
β-ODAP
GluOx
0.135 V
α-keto -β N-oxalylglutaric acid
2e⁻
Chitosan
AuNPs
cMWCNT
Signal
Glutamate Oxidase (GluOx)
GluOx/AuNP/cMWCNT/CHIT/Au electrode

Fig. 8.

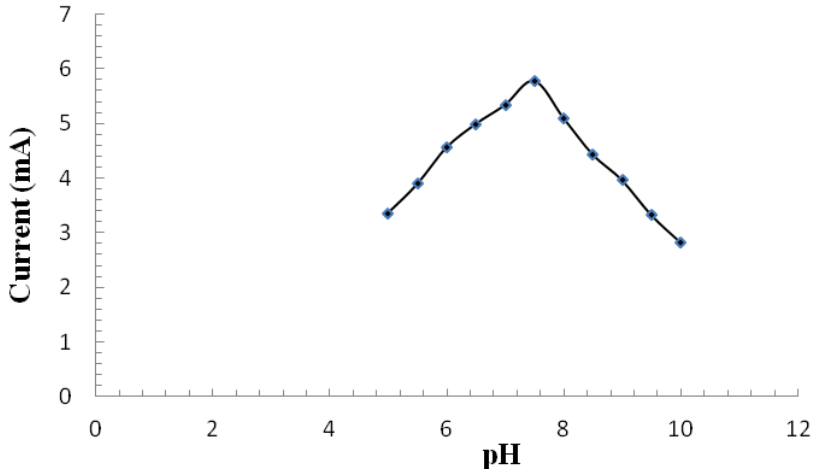
Current (mA)
0
1
2
3
4
5
6
7
0
2
4
6
8
10
12
pH

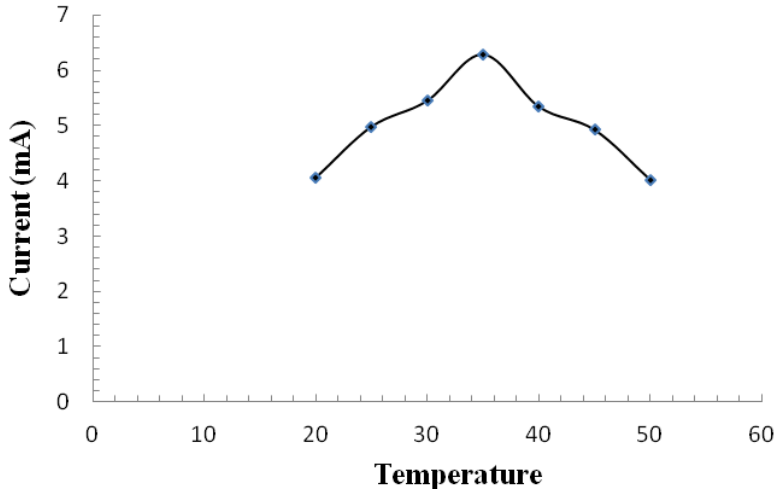
Current (mA)
0
1
2
3
4
5
6
7
0
10
20
30
40
50
60
Temperature

Fig.9.

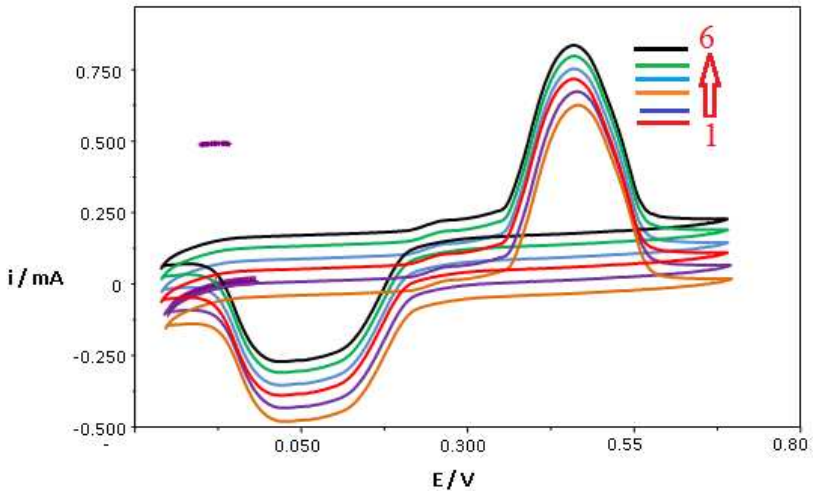

Fig.10.

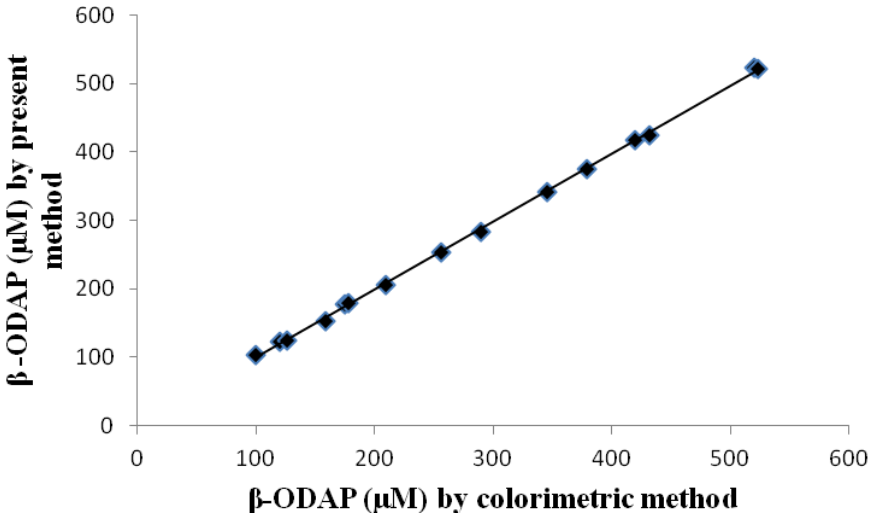
600
500
400
300
200
100
0
0
100
200
300
400
500
600
β-ODAP (μM) by present method
β-ODAP (μM) by colorimetric method

Fig.11.